Performance Evaluation of an Optical Flow Technique applied to Particle Image Velocimetry using the VSJ Standard Images

G. M. Quénot

Abstract. A Dynamic Programming based Optical Flow technique has been applied to the Particle Image Velocimetry (PIV) problem. It has been tested for the search of two-component (using one camera) and three-component (using two or three cameras) planar velocity fields corresponding to a region illuminated by a laser light sheet. Tests have been carried out on calibrated synthetic image sequences from the PIV Standard Project of the Visualization Society of Japan (VSJ). Results are presented for the 2D flow field based sequences (VSJ test sets 01 to 08)and the 3D flow field based sequences (VSJ test sets 301, 302, 331 and 337). Accuracy is within the 2-3 % range and within the 3-5 % range for the two-component and the three-component flow field recovery respectively.

1 Introduction

The experimental fluid mechanics technique of Particle Image Velocimetry (PIV) has proven to be a valuable method for quantitative, two-dimensional flow structure evaluation [1]. It enables the measurement of the instantaneous in-plane velocity vector field within a planar section of the flow field. Using two or more cameras, it is also possible to get the out-of-plane velocity component. Nowadays, almost all PIV is done by computer image processing on digital images (DPIV) [2] and most methods are based on image intercorrelation.

One of the main drawbacks of classical DPIV is its inability to accurately resolve flow regions characterized by large velocity gradients. This is due to the strong deformation of the particle image pattern within a DPIV search window. Hence, several alternative evaluation methods have been proposed to remove the above limitation [4], [5], [6].

G. M. Quénot
CLIPS-IMAG, B.P. 53, 38041 Grenoble Cedex 9, France

It has been shown [8] that an *optical flow* method [3] [7] may also be an interesting alternative, offering high evaluation accuracy without most of the typical DPIV limitations. Conventionally, this technique was developed for detecting motion of large objects in a real world scene. The idea of this evaluation technique is in some sense similar to the Image Correlation Velocimetry proposed by Tokumaru and Dimotakis [5].

The objective of the present study is to better characterize the performance of the optical flow technique for PIV using publicly available image sequences from the PIV Standard Project of the Visualization Society of Japan [9].

2 Optical Flow for Particle Image Velocimetry

Optical flow computation consists in extracting a dense velocity field from an image sequence assuming that the intensity (or color) is conserved during the displacement. Many techniques have been developed for the computation of optical flow. Not all of these are well suited for the DPIV problem. Many require long image sequences that are not easily obtainable experimentally and/or do not perform very well on the particle image texture (especially multi-resolution methods).

The technique that was chosen for the PIV application was introduced as the Orthogonal Dynamic Programming (ODP) algorithm for optical flow detection from a pair of images [3]. The originality of this algorithm is that it transforms the (complex) search problem for two-dimensional alignments into a carefully selected sequence of (simple) search problems for monodimensional alignments. It is based on an iterative search for a continuous and regular velocity field that brings the second image over the first one while minimizing the L_1 or L_2 (Minkowski) distance between them. The technique has been extended to be able to operate on longer sequences of images and to search for subpixel displacements [7]. The ODP based PIV will

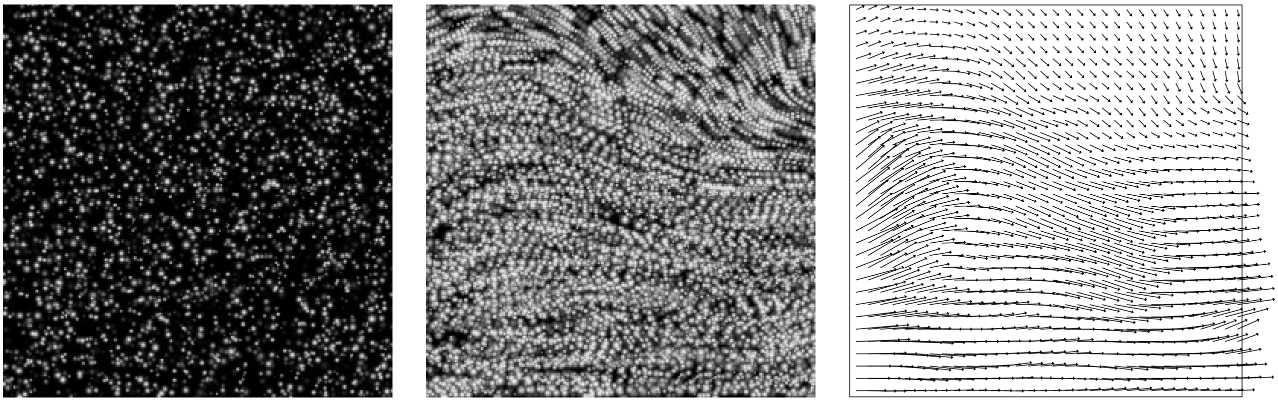

Figure 1: One particle image, four superimposed images and the correct velocity field

be referred to as ODP-PIV. It cannot be detailed here but it is fully explained in [8]; it can be related to classical intercorrelation techniques but with the following differences:

- Basic matching is searched on elastic image strips (either horizontal or vertical) instead of being searched on rigid blocks, and robust strip matching is performed using Dynamic Programming which enforces continuity and regularity constraints,
- A global, dense, continuous and coherent image matching is iteratively updated and refined using alternatively horizontal and vertical strip matchings and by reducing the strips' width and spacing along with the iterations,
- The technique is able to operate on multiband (e.g. color) images,
- It can be applied simultaneously to sequences of more than two images,
- It can search for subpixel displacements,
- It provides dense vector fields (1 velocity vector for every pixel, neither holes nor border offsets).

3 The VSJ PIV-STD Project

A research group (PIV-STD) organized by the Visualization Society of Japan (VSJ) has developed standard image test sets for quantitative performance evaluation and comparison of PIV systems [9]. They are distributed via Internet (`http://www.vsj.or.jp/piv/`) or by CDROM and publicly available. "Standard" image sequences are proposed for 2D and 3D flows. The results presented here make use of standard image sequences based on 2D flows (test sets 01 to 08), and 3D flows both for the recovery of two components (test sets 301 and 302) and three components (test sets 331 and 337) of the velocity fields in a planar section of the flow.

4 Recovering 2D flows

The first standard image sequence (s01) is a "typical" case defined by the following parameters : N = 4000 (number of particles), T = 33 ms (time interval, defining the scale of the in-plane velocity), v = 7.39 pixel/interval (in-plane velocity), L = 20.0 mm (light sheet thickness, defining the scale of the out-of-plane velocity), w = 0.017 -/interval (out-of-plane velocity, fraction of the particles leaving and entering the light sheet per interval), P_a = 5.0 pixel (average particle diameter) and P_d = 1.4 pixel (standard deviation of particle diameter). The seven following standard image sequence (s02 to s08) differ from the typical case by only one parameter. The images are 256 × 256 pixels representing an actual 100 mm × 100 mm area. The ratio between the in-plane and out-of-plane average velocities is of about 0.12 (defining a 2D flow). Figure 1 shows one image of the first sequence, four consecutive superimposed images and the used velocity field.

Table 1 displays the parameter set used for the eight standard sequences as well as the accuracy results for the ODP-PIV method using respectively two, three and four images. ODP-PIV control parameters are tuned differently for low and high out-of-plane velocity (s08 sequence). The PIV-STD group does not specify any particular way of displaying

No.	N	T	v	L	w	P_a	P_d	2 images	3 images	4 images
s01	4000	33	7.39	20.0	0.017	5.0	1.4	3.52±2.91	3.29±2.74	3.21±2.66
s02	4000	**100**	22.4	20.0	0.053	5.0	1.4	10.8±11.7	10.2±10.2	10.2±10.5
s03	4000	**10**	2.24	20.0	0.005	5.0	1.4	9.82±5.14	9.74±5.00	9.75±4.96
s04	**10000**	33	7.39	20.0	0.017	5.0	1.4	1.97±2.67	1.45±1.82	1.33±1.53
s05	**1000**	33	7.39	20.0	0.017	5.0	1.4	3.53±3.42	2.68±3.14	2.33±2.98
s06	4000	33	7.39	20.0	0.017	5.0	**0.0**	2.30±4.13	1.50±1.57	1.33±1.41
s07	4000	33	7.39	20.0	0.017	**10.**	4.0	2.93±4.51	2.23±2.95	2.08±2.89
s08	4000	33	7.39	**2.0**	0.176	5.0	1.4	7.79±13.0	5.05±4.57	3.90±3.82

Table 1: Results on the VSJ standard sequences 01 to 08

the results or any comparison program. Accuracy results are displayed here in *percentage* as mean error ± standard deviation of error, the error being the relative error (absolute error in pixel/interval divided by the average in-plane velocity also in pixel/interval).

The typical case parameters appear to be suboptimal for the ODP-PIV method (they are probably tuned for Particle Tracking methods) for the particle density (at least 2.5 times too small) and size (twice too big). However, the default in-plane velocity scale is near the optimum and the out-of-plane velocity has negligible effect (except for the s08 sequence).

The accuracy for the typical case (s01) is below 4 % for the three variants. Severe accuracy degradation occurs when the average in-plane velocity is far (3 times smaller or larger, s02 and s03) from the optimum one. Increasing the particle density (s04) highly improves the accuracy while decreasing again the particle density (s05) does not further degrade the accuracy. Reducing the particle diameter standard deviation improves the accuracy (s06) as well as incresing the particle diameter (s07, however this is linked to the insufficient particle density). Finally, high out-of-plane velocity (s08, 17 % of particle appearance and disappearance per interval) significantly degrades the accuracy. However, even in this case, an accuracy of about 4 % is obtained using the four images. Near the optimal particle density (s04), the accuracy is as good as 2 % using only two images and below 1.5 % using the four images.

Custom image sequences were also generated using the version 2 of the custom made standard image program in order to evaluate the effect of the various tunable parametrs [10]. These image sequences are also publicly available from the VSJ server from: `http://www.vsj.or.jp/piv/java/tmp2/-<No.>/index.html`. The `<No.>` field is to be replaced by the corresponding test set number (100 to 114).

The optimal number of particles for the method is 10000 (one particle by 6.4 square pixels density), which is the maximum allowed by the sequence generation program. However, it is estimated from the data that the optimal density without that limitation would be about the same. The optimal particle diameter is around 2.5-3.0 pixel. The optimal average in-plane velocity is of about 8-9 pixel/interval. This last value may change for higher relative out-of-plane velocities (w, a value of 0.05 is used here).

5 Recovering two components of 3D flows

Recovering two components of 3D flows is almost the same problem as the recovering of 2D flows. Two components only (the in-plane ones) are recovered from a single camera. The third component, however, is no longer supposed to be negligible; it is not recovered but makes the problem more difficult by inducing much higher rates of particle appearance and disappearance.

Test set 301 contains a single 145-image continuous sequence (of a jet impinging on a wall at 12 cm/s with a Reynolds number of 3000, the time step is 5 ms) as well as the correct flow field for each time step. The target flow field is a 4cm × 4cm × 2cm volume and the laser light sheet thickness is 2mm (with a gaussian profile). The average number of particles in images (256 × 256) is 4000 and the average particle diameter is of 5 pixels with a standard deviation of 2 pixels. Test set 302 is identical to test set 301 except that the average number of particles in images is 1000 instead of 4000.

Flow fields have been recovered from the sequences for all possible time steps using from 2 to 7 consecutive images and compared to the corresponding correct one. Table 2 displays the errors again in percentage (mean of the module of the difference between the recovered and correct flow fields divided by the mean of the module of the correct flow field). The errors are computed for every possible time step in the sequence and the minimum, average and maximum values are displayed for both sequences. The minimum, average and maximum values of the w parameter (specifying the average percentage of particles entering and leaving the light sheet at each time step) are respectively of 3.67 %, 6.08 % and 8.52 % (to be compared to 1.76 % for the standard typical "2D" case).

used	std301 (4000 part.)			std302 (1000 part.)		
images	min.	avg.	max.	min.	avg.	max.
2	3.53	4.86	6.24	4.94	6.84	8.91
3	2.57	3.73	4.96	3.86	5.73	7.69
4	2.25	3.16	4.04	3.50	5.08	6.54
5	1.85	2.75	3.58	3.18	4.75	6.09
6	1.80	2.69	3.29	3.09	4.53	5.70
7	1.93	2.86	3.67	3.10	4.67	5.83

Table 2: Results on the VSJ sequences 301 and 302

It must be noticed that the parameters chosen for the virtual PIV experimental setup here are not the optimal ones for the ODP-PIV method as it has been mentioned in the previous section. For the recovery of the same flow field, significantly better results could probably be achieved using more smaller particles (and maybe a slightly larger time step), but the possibility to generate custom sequences with tuning of these parameters like in the 2D case does not currently exist for the 3D sequences.

6
Recovering three components of 3D flows

Stereo PIV is used to recover also the third component of the velocity vectors. Figure 2 shows the stereo PIV virtual experimental setup used. Images are taken simultaneaously from three different cameras, all three being 6cm far from the center of the visualized flow field: camera 1 is centered and camera 0 and 2 are respectively 30 degrees off on the left and on the right. The target flow field is a 4cm × 4cm × 2cm volume and the visualized flow field is a 1.2cm × 1.2cm × 0.2cm volume (with a gaussian laser light sheet profile) for the std331 test set and a 2cm × 2cm × 0.2cm volume for the std337 test set. Also, the flow field is assumed to be in water ($n = 1.33$) while cameras are in air ($n = 1.00$), both being separated by a wall at 3cm from the visualized flow field. The average number of particles in images (256 × 256 pixels) is 4000 and the average particle diameter is of 5 pixels with a standard deviation of 2 pixels.

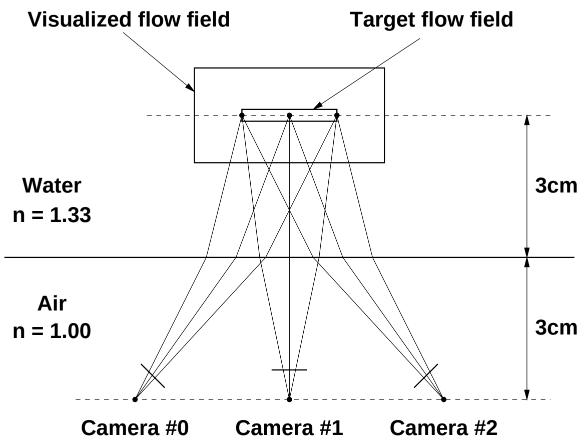

Figure 2: Stereo PIV virtual experimental setup (top view)

Test set 331 contains three 145-image continuous sequence (of a jet impinging on a wall at 15 cm/s with Reynolds number of 3000, the time step is 5 ms) taken by the three cameras (Figure 3). Test set 337 is identical to test set 331 except that : the sequences are 201-image long each, the time step is 2 ms, and the visualized flow field is different as mentioned in the previous paragraph The exact 3D vector field to be recovered is also provided for comparison (Figure 4).

Compared to the two-component case, the computation process has three steps here: computation of the apparent 2D flow field for each camera, alignment of these 2D flow fields on the planar search area, and building a single three-component vector from two or three two-component vectors (for each desired location). The first step is identical to the classical two-component search (using 7 consecutive images). The two following steps consist in simple geometric transformations that make use of the camera calibrations. The last step also makes use of a least square method.

Table 3 shows the accuracy results for the recovery of one three-component flow field using data from only two or all three cameras for each test set. Test set 337 has a greater out of plane (3D) component than test set 331, which explains its lower accuracy. The relative error is within the 3-5% range when all available information is used (seven images from all three cameras). However, suppressing the information from the center camera does not significantly degrade the result.

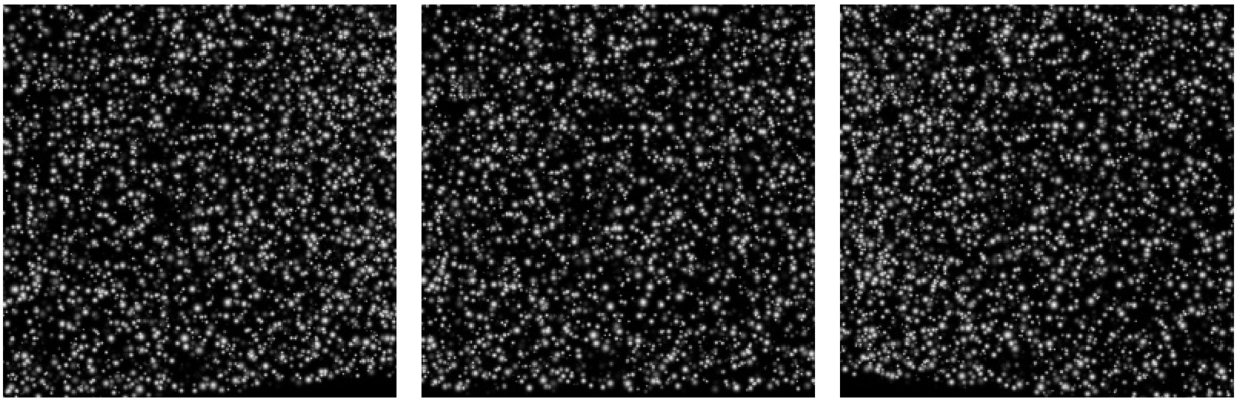

Figure 3: Images from the VSJ sequence 337: left, center and right cameras.

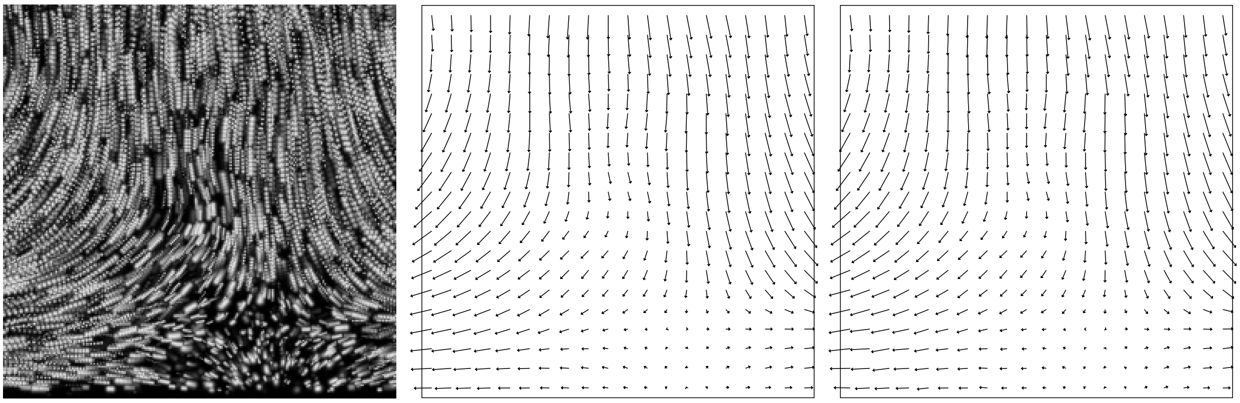

Figure 4: Vector fields from the VSJ sequence 337, from left to right: 7 superimposed images from center camera, correct flow field (xy), recovered flow field (xy). Though not displayed here, the third flow field component (z) is also recovered.

Vector field to be recovered	331/vec003.dat				337/vec003.dat			
Mean x correct velocity (cm/s)	1.86				3.98			
Mean y correct velocity (cm/s)	9.13				8.82			
Mean z correct velocity (cm/s)	1.71				3.83			
Mean xy correct velocity (cm/s)	9.82				11.6			
Mean xyz correct velocity (cm/s)	10.0				12.5			
Recovered from sequences	(1,2)	(0,2)	(0,1)	(0,1,2)	(1,2)	(0,2)	(0,1)	(0,1,2)
Mean x velocity error (cm/s)	0.14	0.11	0.14	0.12	0.17	0.15	0.17	0.13
Mean y velocity error (cm/s)	0.14	0.13	0.10	0.11	0.22	0.21	0.23	0.20
Mean z velocity error (cm/s)	0.18	0.16	0.23	0.16	0.53	0.40	0.52	0.40
Mean xy velocity error (cm/s)	0.26	0.23	0.23	0.22	0.38	0.35	0.40	0.34
Mean xyz velocity error (cm/s)	0.35	0.31	0.38	0.30	0.81	0.64	0.80	0.64
Mean x velocity relative error (%)	1.38	1.12	1.39	1.17	1.33	1.18	1.37	1.07
Mean y velocity relative error (%)	1.40	1.34	1.03	1.11	1.78	1.66	1.85	1.64
Mean z velocity relative error (%)	1.83	1.60	2.31	1.60	4.28	3.19	4.13	3.19
Mean xy velocity relative error (%)	2.60	2.29	2.25	2.17	3.07	2.82	3.21	2.74
Mean xyz velocity relative error (%)	3.46	3.13	3.79	3.04	6.47	5.15	6.40	5.10

Table 3: Accuracy results for the stereo ODP-PIV on the VSJ sequences 331 and 337

Again, the parameters chosen for the virtual PIV experimental setup here are not the optimal ones for the ODP-PIV method as it has been mentioned in the previous sections and, for the recovery of the same flow field, significantly better results could probably be achieved using more smaller particles.

7 Conclusion

This work has shown that the ODP Optical Flow technique is very efficient for the recovery by Particle Image Velocimetry in a planar section of two or three velocity components of three-dimensional flows. Its accuracy is within the 2-3 % range for the two-component recovery and within the 3-5 % range for the three-component recovery (on the test sets 01 to 08, 301, 302, 331 and 337 of the PIV-STD project of the Visualization Society of Japan).

However, these results have been obtained using the exact camera calibration for the three-component serch (not a recovered one). Taking into account camera calibration would certainly increase the error in the flow fied recovery.

Also, the PIV-STD synthetic images and very clean (without any noise) and, in this regard, may not be as representative of real data as it would be desirable. Though they are useful for comparing, on a quantitative and objective ground, the relative performances of PIV systems and for providing an estimation of their absolute performances, results might change significantly with real and noisy data. Therefore, experiments should also be conducted using real PIV data. The ODP-PIV has been proven to be very robust to noise using other synthetic data with noise and real data [8], also publicly available for comparative performance evaluation from the LIMSI web site at: `ftp://ftp.limsi.fr/-pub/quenot/opflow/testdata/piv`.

Future work will consider the effects of both approximate camera calibration and noise for the performance evaluation of the ODP-PIV method and other methods using both synthetic and real data.

References

[1] Hesselink L.: Digital Image Processing in Flow Visualization, *Ann. Rev. Fluid Mech.,* Vol. 20, pp. 421-485, 1988.

[2] Willert C.E., Gharib M.: Digital particle image velocimetry, *Experiments in fluids*, Vol 10, pp. 181-193, 1991.

[3] Quénot G.M.: The "orthogonal algorithm" for optical flow detection using dynamic programming, *Intl. Conf. on Acoustics, Speech and Signal Proc.*, pp. 249–52, San Francisco CA, 23-26 mar. 1992

[4] Huang H.T, Fiedler H.E, and Wang J.J.: Limitation and improvement of piv. part i: Limitation of conventional techniques due to deformation of particle image patterns. *Exp Fluids*, Vol. 15, pp 168–174, 1993.

[5] Tokumaru P.T. and Dimotakis P.E. Image correlation velocimetry. *Exp Fluids*, Vol. 19, pp 1–15, 1995.

[6] Merzkirch W. and Gui L.C. A method of tracking ensembles of particle images. *Exp Fluids*, Vol. 21, pp 465–468, 1996.

[7] Quénot G.M.: Computation of Optical Flow Using Dynamic Programming, *IAPR Workshop on Machine Vision Applications,* pp. 249-52, Tokyo, Japan, 12-14 nov. 1996.

[8] Quénot G.M., Pakleza J., Kowalewski T.A.: Particle Image Velocimetry with Optical Flow, *Experiments in fluids*, Vol. 25, No. 3, pp. 177-189, 1998.

[9] Okamoto K., Nishio S., Kobayashi T., Saga T.: Standard Images for Particle Image Velocimetry, *Proc. of the Second Inter. Workshop on PIV*, Fukui, Japan, pp. 229-236, 1997.

[10] Quénot G.M.: Performance Evaluation of an Optical Flow for Particle Image Velocimetry, *Euromech Colloquium on Image Processing in Applied Mechanics*, pp 177-180, Warsaw, Poland, 6-8 May, 1999.